THE JOURNAL OF BIOLOGICAL CHEMISTRY VOL. 282, NO. 37, pp. 26948–26955, September 14, 2007

Engineered Sarafotoxins as Tissue Inhibitor of Metalloproteinases-like Matrix Metalloproteinase Inhibitors*

Received for publication, December 19, 2006, and in revised form, July 5, 2007 Published, JBC Papers in Press, July 10, 2007, DOI 10.1074/jbc.M611612200

Janelle L. Lauer-Fields[‡§], Mare Cudic[§], Shuo Wei[‡1], Frank Mari[§], Gregg B. Fields[§], and Keith Brew[‡2]

From the [‡]College of Biomedical Science and [§]Department of Chemistry & Biochemistry, Florida Atlantic University, Boca Raton, Florida 33431

The sarafotoxins and endothelins are ~25-residue peptides that spontaneously fold into a defined tertiary structure with specific pairing of four cysteines into two disulfide bonds. Their structures show an interesting topological similarity to the core of the metalloproteinase interaction sites of the tissue inhibitors of metalloproteinases. Previous work indicates that sarafotoxins and endothelins can be engineered to eliminate or greatly reduce their vasopressive action and that their structural framework can withstand multiple sequence changes. When sarafotoxin 6b, which possesses modest matrix metalloproteinase inhibitory activity, was C-terminally truncated to remove its toxic vasopressive activity, the metalloproteinase inhibitory activity was essentially abolished. However, further changes, based on the sequences of peptides selected from libraries of sarafotoxin variants or suggested by analogy with tissue inhibitors of metalloproteinases, progressively enhanced the matrix metalloproteinase inhibitory activity. Peptide variants with multiple substitutions folded correctly and formed native disulfide bonds. Improvements in matrix metalloproteinase affinity have generated a peptide with micromolar K_i values for matrix metalloproteinase-1 and -9 that are selective inhibitors of different metalloproteinases. Characterization of its solution structure indicates a close similarity to sarafotoxin but with a more extended C-terminal helix. The effects of *N*-acetylation and other changes, as well as docking studies, support the hypothesis that the engineered sarafotoxins bind to matrix metalloproteinases in a manner analogous to the tissue inhibitors of metalloproteinases.

The endothelins (ET)[3] are a family of 21–25-residue peptides that fall into two major categories, endothelins and sarafotoxins (Srt). The names are derived from their biological sources, endothelial cells, and the venoms of snakes of the genus *Atractaspis* (in Hebrew, *Saraf Ein Gedi*). Three ETs are found in humans, and an array of Srts are present in the venoms of different *Atractaspis sp*. ET family complexity arises from a variety of mechanisms; expression from multiple genes, proteolytic processing, and possibly RNA editing (1–4). NMR and crystallographic studies reveal that these peptides contain a bicyclic two-disulfide (Cys^1–Cys^{15}, Cys^3–Cys^{11}) framework with a specific tertiary structure. The N-terminal residues form a β-strand followed by a β-turn at residue 5 (5); residues 9–16 are mainly α-helical, whereas the C-terminal residues are flexible in solution (6). However, the crystal structure and protease susceptibility studies suggest that these C-terminal residues may associate with the bicyclic core as an α-helix (7, 8).

ETs have many physiological effects including stimulation of cell proliferation, promotion of the expression of cell adhesion molecules and extracellular matrix components, activation of the inflammatory cascade, and the well characterized contraction of smooth muscle tissue (9). In humans, these biological activities are mediated via the endothelin receptors, ET_A and ET_B. ET_B receptors bind ETs and Srts with little selectivity, whereas ET_A receptors show greater affinity for ET-1, ET-2, and Srt b, over ET-3 and Srt c (5). The flexible C-terminal hexapeptide residues, especially Trp^{21}, have been found to be critical for high affinity binding to ET_A and ET_B (10), and truncated peptides containing this region in isolation are effective antagonists of ET binding to both receptor types (5).

The tissue inhibitors of metalloproteinases (TIMPs) are a group of high affinity endogenous inhibitors of the matrix metalloproteinases (MMPs) and some disintegrin metalloproteinases (ADAM and ADAMTSs). TIMPs have an integral role in regulating MMP activities, and an appropriate balance between TIMPs and active MMPs is crucial for ECM homoeostasis. Active MMPs have important physiological roles in embryonic development and wound healing, but excess MMP activity has been linked to pathological conditions including arthritis, cardiovascular disease, and tumor cell metastasis (11). Because the TIMPs play a key role in modulating metalloproteinase activity, they offer a potential route for therapeutic intervention in these diseases (11–13). The four TIMPs found in mammals (TIMP-1–4) have overlapping inhibitory specificities and together regulate the activities of more than 30 metalloproteinases in humans (11). Mammalian TIMPs are two-domain molecules, having a larger N-terminal domain (~120 amino acids) and a smaller C-terminal domain of ~65 residues; each domain is stabilized by three disulfide bonds. The MMP inhibitory activ-

* This work was supported by National Institutes of Health Grants AR 40994 (to K. B.) and CA 98799 (to G. B. F.) and by a grant from the American Federation for Aging Research (to J. L. L.-F.). This work was also supported in part by National Institutes of Health Grant P41 RR-001081. The costs of publication of this article were defrayed in part by the payment of page charges. This article must therefore be hereby marked "*advertisement*" in accordance with 18 U.S.C. Section 1734 solely to indicate this fact.

[1] Present address: Dept. of Cell Biology, University of Virginia Health Sciences Center, P.O. Box 800732, Charlottesville, Virginia 22908.

[2] To whom correspondence should be addressed: College of Biomedical Science, Florida Atlantic University, 777 Glades Rd., Boca Raton, FL 33431. Tel.: 561-297-0407; Fax: 561-297-2221; E-mail: kbrew@fau.edu.

[3] The abbreviations used are: ET, endothelin; Abu, aminobutyric acid; ADAM, a disintegrin and metalloproteinase; MALDI-TOF MS, matrix-assisted laser desorption ionization time-of-flight mass spectrometry; MMP, matrix metalloproteinase; NEM, N-ethylmaleimide; N-TIMP, N-terminal domain of tissue of inhibitor of metalloproteinases; TIMP, tissue inhibitor of metalloproteinases; RP, reversed phase; HPLC, high performance liquid chromatography; Srt, sarafotoxin; STX, sarafotoxin 6b truncated at Asp^{18}; Fmoc, *N*-(9-fluorenyl)methoxycarbonyl; NOE, nuclear Overhauser effect.

ity is located in the N-terminal domain and recombinant forms of the truncated N-terminal domains of TIMPs (N-TIMPs) fold independently and are fully active as metalloproteinase inhibitors (11). The crystallographic structure of the TIMP-1/MMP-3 complex indicated that ~75% of the intermolecular contacts of the TIMP-1 component with MMP-3 are made by the residues surrounding the Cys^1–Cys^{70} disulfide bond, specifically residues 1–5 and 66–70 (14). Similar contacts were observed subsequently in the structure of complexes of TIMP-2 with MMP-14 (15) and MMP-13 (16) and the complex of N-TIMP-1 with MMP-1 (17). To develop their potential as therapeutic agents while minimizing deleterious side effects, N-TIMPs have been successfully engineered by mutation of their MMP interaction sites to enhance their inhibitory selectivity for different metalloproteinases (18–20). However, there are many advantages associated with engineering a smaller peptide inhibitor of metalloproteinases if a TIMP-like scaffold can be identified. In relation to this possibility, we noticed a topological similarity between ETs and the core of the MMP interaction site of TIMP (see Fig. 1).

ETs and Srts are generated *in vivo* by proteolytic cleavage from larger precursors. However, previous studies have shown that they can be produced by solid phase peptide synthesis and fold spontaneously *in vitro* in high yield into native tertiary structures with the correct disulfide bond pairing of cysteines. Also, a number of ET variants have been produced that retain the ability to fold correctly (21–24), suggesting that the ET scaffold is robust and is an appropriate starting point for the design of small topologically defined peptides with possible metalloproteinase inhibitory activities. Our initial studies showed that Srt6b has some inhibitory activity toward MMP-2 and MMP-3 leading to an investigation of peptides based on Srt6b that are modified to greatly reduce or eliminate their potentially toxic vasopressive activity. Although initial changes of this type also largely eliminated MMP inhibitory activity, we were able to incorporate further changes that enhance selective inhibitory activity toward MMPs, producing inhibitors with K_i values of ~1 μM. Structural characterization by circular dichroism and NMR indicates that the inhibitors have solution structures that are similar to Srt and ET but with increased helical content. The effects of structural changes and molecular docking studies support the view that Srt variants may act in a manner analogous to TIMPs.

MATERIALS AND METHODS

All of the standard chemicals were peptide synthesis or molecular biology grade and were purchased from Fisher. 2-(1H-benzotriazole-1-yl)-1,1,3,3-tetramethyluronium hexafluorophosphate, 1-hydroxybenzotriazole, and Fmoc amino acid derivatives were obtained from Novabiochem (San Diego, CA). The substrates for MMP assays, NFF-3 (Mca-RPKPVE-Nva-WRK(Dnp)-OH) for MMP-3 and Knight substrate (Mca-KPLGL-K(Dnp)AR-NH_2) for MMP-1, MMP-2, MMP-9, and MMP-14, were prepared and characterized as described (25, 26). The ADAM-17 substrate (Mca-PLAQAV-Dpa-RSS-NH_2) was purchased from R & D Systems (Minneapolis, MN). The ADAMTS-4 substrate, which incorporates an ELE↓GR cleavage motif has been described previously (27).

Peptide Synthesis—Peptide-resin assembly was performed by Fmoc solid phase methodology on an ABI 433A peptide synthesizer (28). Cleavage and side chain deprotection of peptide-resins proceeded for at least 2 h using Reagent K, phenol-thioanisole-water-ethanedithiol-trifluoroacetic acid (5:5:5:2.5:82.5) (29). Cleavage solutions were extracted with methyl *t*-butyl ether prior to purification. Limited combinatorial libraries of peptides were generated by mixing Fmoc-protected amino acids in appropriate ratios to produce equimolar coupling based on the work of Ostresh *et al.* (30).

Peptide Folding and Purification—Crude peptides were dissolved in 1 mM 2-hydroxyethyl disulfide, 5 mM 2-mercaptoethanol in 0.1 M NH_4HCO_3, pH 8.5, and mixed 1–18 h at 4 °C. Disulfide bond formation was monitored by analytical RP-HPLC based on the observation that oxidized endothelin model peptides elute earlier than reduced peptides (18, 23). RP-HPLC was performed with a Hewlett-Packard 1100 liquid chromatograph equipped with a Vydac 218TP5415 C_{18} RP column (5-μm particle size, 300-Å pore size, 150 × 4.6 mm). Eluants were 0.1% trifluoroacetic acid in water (Solvent A) and 0.1% trifluoroacetic acid in acetonitrile (Solvent B). The column was eluted with a gradient from 0–60% B in 25 min at a flow rate of 1.0 ml/min, and eluted peptides were detected by UV absorbance at $\lambda = 220$ and 280 nm. The peptides were purified using a Rainin Auto-Prep system with a Vydac C_{18} column (15–20-μm particle size, 300-Å pore size, 250 × 22 mm) at a flow rate of 10.0 ml/min using the same eluants; the elution gradient was adjusted as required. Most of the cysteine-containing peptides folded into two forms separable by RP-HPLC. The earlier eluting fraction was found to contain the correctly folded peptide. Thus, fractions containing homogenous products were identified by a combination of analytical RP-HPLC and MALDI-TOF MS.

Peptide Characterization—MALDI-TOF MS was performed with an Applied Biosystems Voyager DE-STR MALDI-TOF mass spectrometer using an α-cyano-4-hydroxycinnamic acid matrix (31). Sulfydryl content was determined with 5-5′-dithiobis(2-nitrobenzoic acid) using a D/L-cysteine standard curve (32, 33). Disulfide bond connectivity was assigned by partial reduction using tris(2-carboxyethyl) phosphine and derivatization with *N*-ethylmaleimide (NEM) (34). Briefly, a sample (9 nmol) of peptide was reduced for 5 min with a 25–50-fold excess of tris(2-carboxyethyl) phosphine in 0.1 M citrate, pH 3.0. Sulfhydryls were derivatized using a 600-fold excess of NEM in 0.1 M citrate, pH 3.0, for 20 min followed by immediate RP-HPLC purification. Fractions corresponding to partially reduced peptide were analyzed by MALDI-TOF MS and by automated Edman degradation with an ABD Procise 494 Sequencer. Far UV (λ = 195–250 nm) circular dichroism spectra were measured with a JASCO J-810 spectropolarimeter using a 0.1-cm-path length quartz cell. Temperature was controlled using a JASCO PFD-425S temperature control unit. CD spectra were analyzed using the k2d neural network program (35) to predict the secondary structure content of peptides.

Affinity Chromatography—The chosen metalloproteinase was coupled to NHS-Sepharose (GE Biosciences) following the manufacturer's protocol. All of the bound enzymes retained activity. A combinatorial peptide library was mixed with immobilized enzyme overnight at 4 °C. Weakly or nonspecifically

bound peptides were removed with 3 column volumes of enzyme buffer (50 mM Tris, 100 mM NaCl, 10 mM $CaCl_2$, 0.05% Brij-35, pH 7.5), and bound peptides were eluted serially in 5 column volumes of 20% isopropanol. Each fraction was analyzed by MALDI-TOF MS to identify bound peptides.

Matrix Metalloproteinases—Full-length proMMP-1 and a truncated form of proMMP-3 missing the C-terminal hemopexin domain were expressed in *Escherichia coli* and folded from inclusion bodies as described previously (36). ProMMP-1 was activated using 1 mM 4-aminophenylmercuric acetate and 0.02 eq of MMP-3 at 37 °C for 6 h. After activation, MMP-3 was separated from MMP-1 by affinity chromatography with a column of anti-MMP-3 IgG Affi-Gel 10. ProMMP-3 was activated by treatment with 5 μg/ml chymotrypsin at 37 °C for 2 h. Chymotrypsin was then inactivated with 2 mM diisopropylfluorophosphate. ProMMP-2 was purified from the culture medium of human uterine cervical fibroblasts (37) and activated by incubating with 1 mM 4-aminophenylmercuric acetate for 1 h at 37 °C. The concentrations of active MMPs were determined by active site titration with N-TIMP-1 (38). MMP-9 (catalytic domain) was expressed as described elsewhere.[4] EBNA-293 cells expressing ADAMTS-4 were a generous gift of Dr. Hideaki Nagase (The Kennedy Institute for Rheumatology, Imperial College, London). The cells were cultured in Opti-MEM-1 medium with 4% fetal bovine serum, 25 units/ml penicillin, 25 μg/ml streptomycin, 100 μg/ml hygromycin, and 250 μg/ml G418 sulfate (Invitrogen) (39). Conditioned medium was collected, and ADAMTS-4 was purified using an anti-FLAG affinity column followed by size exclusion chromatography using an S75 high load 16/60 Sephacryl column (GE Biosciences). Recombinant MT1-MMP and ADAM-17 were purchased from Chemicon International (Temecula, CA) and R & D Systems (Minneapolis, MN), respectively.

Inhibition Kinetic Studies—Peptide substrates and inhibitors were dissolved in TNC buffer (50 mM Tris-HCl, pH 7.5, containing 100 mM NaCl, 10 mM $CaCl_2$, 0.05% Brij-35, pH 7.5). 1–2 nM enzyme was incubated with varying concentrations of inhibitors for 2 h at room temperature. Residual enzyme activity was monitored by adding 0.1 volume of the appropriate substrate to produce a final concentration of $<0.1\ K_m$. Initial velocity rates were determined from the first 20 min of hydrolysis when product release is linear with time. Fluorescence was measured on a Molecular Devices SPECTRAmax Gemini EM Dual-Scanning Microplate Spectrofluorimeter using $\lambda_{excitation}$ = 324 nm and $\lambda_{emission}$ = 393 nm. Apparent K_i values were calculated using SigmaPlot® by fitting data to the equation $v = v_0/(1 + I/K_i)$, here v_0 is the activity in the absence of inhibitor, and K_i is the apparent inhibition constant. Because the substrate concentration is less than $K_m/10$, the apparent K_i values are insignificantly different from true K_i values. After 18 h, each enzyme-inhibitor pair was monitored by RP-HPLC to test for hydrolysis of the inhibitor. No inhibitor degradation was observed in any case.

NMR Methods—NMR spectra were acquired on a Varian Inova 500 MHz instrument equipped with pulsed-field gradient, 3xRF channels, and waveform generators. The peptides were dissolved at a 2.5 mM concentration in water with 10% D_2O (used for locking purposes) and 4 nmol of TSP and placed in 3-mm NMR tubes (Kontes Glass). The pH was adjusted to 3.6 using 0.01 M NaOH and a Thermo micro-pH probe. The spectra were obtained using a 3-mm HCN generation 5 high performance probe. NMR experiments were conducted at temperatures ranging from 0 to 50 °C to achieve the best chemical shift dispersion to aid the sequence-specific assignments. For one-dimensional NMR experiments, the water signal was suppressed using double spin echo (40). For two-dimensional experiments, water suppression was carried out using WATERGATE (41) in combination with 3919 purge pulses with flip-back (42), which were implemented in the total correlation spectroscopy and NOE spectrometry pulse sequences. All of the two-dimensional NMR spectra were recorded in the phase-sensitive mode using the States-Haberkorn method (43) with a spectral width of 6000 Hz and 2K data points. All of the NMR data were processed using VNMR 6.1C (Varian NMR Instruments) on a Sun Blade 150 work station. Free induction decays were apodized with a shifted sine bell window function and linearly predicted to 1 K points in $t1$ and zero-filled to 2000 × 2000 data matrices. The data were base line-corrected in $F2$ by applying a polynomial function. NOE spectrometry cross-peaks were assigned and classified according to their intensities as strong, medium, or weak with the aid of their volume integrals. Sequence-specific assignments of all proton resonances were carried out using standard biomolecular NMR procedures (44).

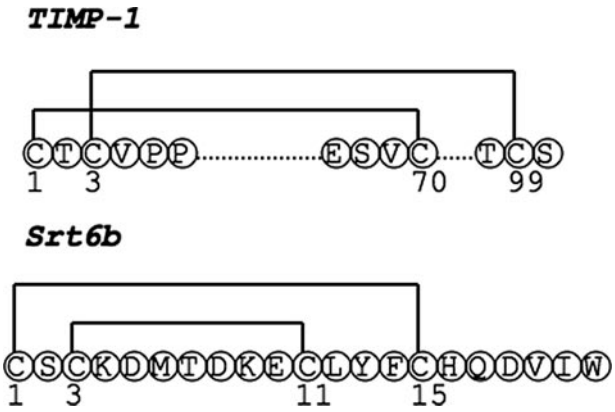

FIGURE 1. **A comparison of disulfide topology and sequences of human N-TIMP-1 and sarafotoxin 6b.**

RESULTS

A member of the ET family whose solution structure has been determined (6, 45), sarafotoxin 6b (Srt6b) (Fig. 1), was initially tested for MMP inhibitory activity and was found to inhibit MMP-2 and MMP-3 with K_i values of 4 and 8 μM, respectively (data not shown). To decrease the affinity for the endothelin receptors and thus reduce or eliminate other biological activities and toxicity, Srt6b was truncated at Asp^{18}. This peptide, designated STX, lost essentially all of its inhibitory activity toward MMPs but was used as a starting point for developing metalloproteinase inhibitors (for nomenclature and sequences, see Table 1). Initially, positions 4 and 16 were cho-

[4] Hamze, A., Wei, S., Bahudhanapati, H., Kota, S., Acharya, K. R., and Brew, K. (2007) *Protein Sci.* DOI: 10.1110/ps072978507.

TABLE 1
Sequences of sarafotoxin analogs

Name	Sequence
Srt6b	Cys Ser Cys Lys Asp Met Thr Asp Lys Glu Cys Leu Tyr Phe Cys His Gln Asp Val Ile Trp
STX	Cys Ser Cys Lys Asp Met Thr Asp Lys Glu Cys Leu Tyr Phe Cys His Gln Asp
STX-V16	Cys Ser Cys Lys Asp Met Thr Asp Lys Glu Cys Leu Tyr Phe Cys Val Gln Asp
STX-A4	Cys Ser Cys Ala Asp Met Thr Asp Lys Glu Cys Leu Tyr Phe Cys His Gln Asp
STX-S4	Cys Ser Cys Ser Asp Met Thr Asp Lys Glu Cys Leu Tyr Phe Cys His Gln Asp
STX-CT	Cys Ser Cys Lys Asp Met Thr Asp Lys Glu Cys Leu Tyr Phe Cys Met Ser Glu Met Ser
STX-S4-CT	Cys Ser Cys Ser Asp Met Thr Asp Lys Glu Cys Leu Tyr Phe Cys Met Ser Glu Met Ser

FIGURE 2. **A comparison of the three-dimensional structures of sarafotoxin 6b and human N-TIMP-1.** The sarafotoxin structure represents model 10 of the solution NMR structure (Protein Data Bank code 1SRB), whereas N-TIMP-1 is derived from the TIMP-1 component of the crystallographic structure of the TIMP-1/MMP-3 complex (Protein Data Bank code 1UEA). The structures are displayed using Chimera (54).

sen for modification because, based on the Srt/N-TIMP analogy (Figs. 1 and 2), the residues at these sites differ from those in TIMPs, suggesting that appropriate substitutions could impart a more TIMP-like structure and improve the inhibitory activity; also the amino acids at these sites vary within the ET family, suggesting that substitutions would not perturb the folding capacity of these constructs. STX-A4, incorporating Ala (which is found in this site in TIMP-4) and STX-V16, derived from the analogous site in TIMP-1, were generated, folded, purified, and tested for MMP inhibitory activity. Metalloproteinases were selected to represent different subgroups including a collagenase (MMP-1), two gelatinases (MMP-2 and MMP-9), a stromelysin (MMP-3), membrane-type (MT1-MMP), an ADAM (ADAM-17), and an aggrecanase (ADAMTS-4). STX-V16 showed no improvement in inhibitory capacity compared with STX, whereas STX-A4 showed marked improvement toward MMP-1, -2, and -9 (Table 2). None of the peptides significantly inhibited MT1-MMP, ADAM-17, or ADAMTS-4 (data not shown). Based on these results, a variant containing the substitution of Ser for Lys[4] (representing residue 4 from TIMP-2 and TIMP-3) was synthesized. This analog, STX-S4, showed further enhancement of activity toward MMP-1, -2, and -9, and was inactive toward MT1-MMP, ADAM-17, and ADAMTS-4 (Table 2 and Fig. 3).

The best Srt-derived inhibitor, STX-S4, was still slightly less active than the initial Srt6b prior to C-terminal truncation (K_i values of 21 *versus* 8 μM). To attempt to improve its affinity for MMPs, the sarafotoxin structure was examined in comparison with the structure of the TIMP-1/MMP-3 complex. This suggested that additional contacts might be generated via the C-terminal region of the sarafotoxin-derived peptide. (Fig. 2). The C-terminal region is analogous to residues 65–69 of TIMPs (numbering refers to human TIMP-1), which forms part of the TIMP/MMP contact surface (11, 15–17, 46) but is oriented in the opposite direction. Using sequence information from 13 different TIMPs, a limited combinatorial peptide synthesis scheme was devised. This scheme utilized residues 1–15 from the best MMP inhibitor from initial studies (STX-S4). Within this framework, a variety of C-terminal sequences were introduced to produce possible TIMP-like structures. The amino acids represented in the combinatorial pools were: residue 16 Val, Leu, Met, and Ala; residue 17, Ser and Ala; residue 18, Glu, Ser, and Asp; residue 19, Met, Ser, Asp, and Glu; and residue 20, Ala and Ser. The combinatorial pools were weighted more heavily toward residues found in human TIMPs. Nonmammalian TIMPs are less conserved in this region than the mammalian TIMPs and are less well characterized with regard to their functional properties, so a limited array of residues from nonmammalian TIMPs were included. During synthesis, the ratio of each amino acid was chosen to produce predictable molar coupling efficiencies based on prior combinatorial peptide studies (30). For example, amounts of reagents for residue 16 were chosen to generate 2 eq of Val (from human TIMP-1 and -2), 2 eq of Leu (from human TIMP-3 and -4), and 1 eq each of Met (from *Drosophila* TIMP) and Ala (from other TIMPs). As discussed above, the directionality of the TIMP strand is opposite that of the sarafotoxin strand in this region, and TIMP residue 69 (TIMP-1 numbering) was considered to be equivalent to Srt position 16 and TIMP residue 65 to position 19. Mass spectroscopic analysis showed the presence of species corresponding to all possible masses, although sequence redundancy precluded the positive identification of each individual peptide. The peptide mixture was folded and partially purified by RP-

TABLE 2
Apparent K_i values of Srt variants for different MMPs (μM)

Inhibitor	MMP-1	MMP-2	MMP-3	MMP-9	MT1-MMP	ADAM-17	ADAMTS-4
STX	NA[a]	NA	>100	NA	>100	>100	>100
STX-V16	NA	NA	>100	NA	>100	>100	>100
STX-A4	21.5 ± 0.6	41.8 ± 3.5	>100	24.5 ± 0.9	>100	>100	>100
STX-S4	22.0 ± 2.2	35.0 ± 4.4	>100	29.3 ± 0.0	>100	>100	>100
STX-CT	>100	>100	>100	25.3 ± 3.5	>100	>100	>100
STX-S4-CT	4.5 ± 0.0	21.6 ± 2.2	>100	1.0 ± 0.1	>100	>100	>100
Ac-STX-S4-CT	>100	NA	NA	66.0 ± 4.0	NA	NA	NA
Abu-STX-S4-CT	>100	NA	>100	>100	NA	NA	NA
AcAbu-STX-S4-CT	NA	NA	NA	NA	NA	NA	NA

[a] NA, not applicable.

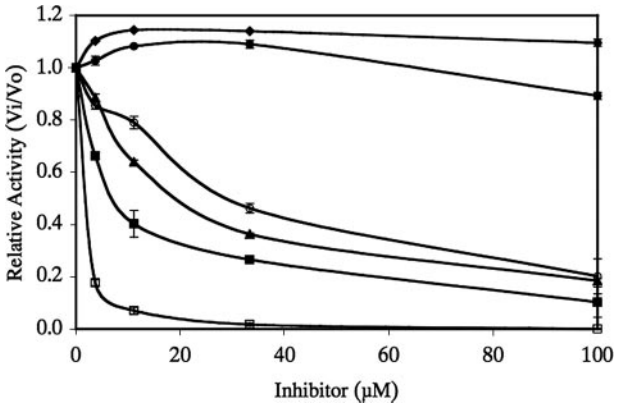

FIGURE 3. **Inhibition profiles of STX variants for MMP-1.** MMP-1 was incubated with varying concentrations of STX (*solid circles*), STX-V16 (*solid diamonds*), STX-A4 (*solid triangles*), STX-S4 (*solid squares*), STX-K4-CT (*open diamonds*), or STX-S4-CT (*open squares*). Residual activity was monitored as indicated under "Experimental Procedures." The standard deviations are indicated with *error bars*.

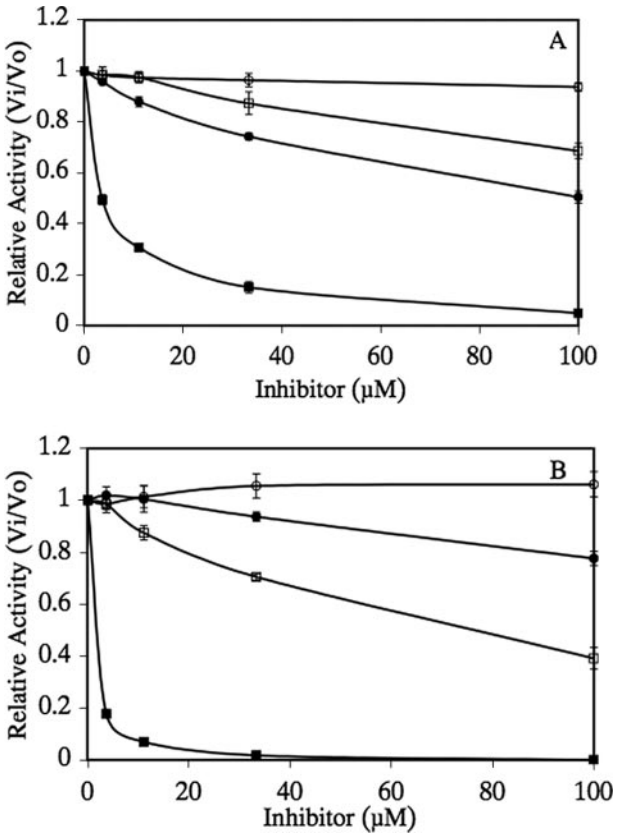

FIGURE 4. **A comparison of the inhibition patterns of STX variants for MMP-1 (*A*) and MMP-9 (*B*).** MMP-1 (*A*) or MMP-9 (*B*) were incubated with varying concentrations of STX-S4-CT (*solid squares*), Ac-STX-S4-CT (*open squares*), Abu-STX-S4-CT (*solid circles*), or AcAbu STX-S4-CT (*open circles*). Residual activity was monitored as indicated under "Experimental Procedures." The standard deviations are indicated with *error bars*.

HPLC. The resulting STX library was applied to an affinity column containing immobilized MMP-1 or MMP-3. Bound peptides were eluted with 5 volumes of 20% isopropanol. MALDI-TOF analysis of the bound fractions indicated the presence of a variety of peptides, of which some could be identified based on mass. One peptide, named STX-S4-CT, bound by both enzymes, was chosen for individual testing. It contained the C-terminal sequence Met-Ser-Glu-Met-Ser, which is not identical with the "equivalent" sequence in any known TIMP. Interestingly, Met^{16} and Ser^{19} correspond to nonmammalian TIMPs (*Drosophila* and *Caenorhabditis elegans*), which were deliberately underrepresented in our original combinatorial library. This peptide was synthesized, folded, purified, and screened for metalloproteinase inhibitory activity; it was found to be a 10–30-fold better inhibitor than STX-S4 (Table 2 and Fig. 3). Interestingly, it also shows modest selectivity between MMP-2 and -9 (22-fold) and between MMP-1 and -9 (4.6-fold). For comparison, a control peptide containing the TIMP-derived C terminus was generated with the original sarafotoxin amino acid (Lys) in position 4, STX-CT. This allowed for the comparison of inhibitory activity arising from the C terminus relative to that derived from the amino acid at position 4. The results suggest that although Ser at position 4 enhances the activity toward MMP-1, -2, -3, and -9, the TIMP-derived C terminus produced some selectivity toward MMP-9 (Table 2 and Fig. 3).

Structure-Function Relationships—An important aspect of the MMP-inhibitory action of TIMP is mediated by the interaction of the α-amino and carbonyl groups of Cys1 of TIMP with the catalytic Zn^{2+} of the protease (14). Modification of the α-amino group by carbamylation or acetylation essentially eliminates the inhibitory activity of TIMP-2 and TIMP-4 toward MMPs (46, 47). To investigate whether Srt model peptides interact in a similar manner with MMPs, an α-*N*-acetylated form of the STX-S4-CT peptide was synthesized (Ac-STX-S4-CT), generating a peptide with approximately a 50-fold weaker MMP inhibitory activity (Table 2 and Fig. 4). Similar results were seen in a N-TIMP-1 mutant incorporating an Ala extension at the N terminus. This protein, called −1Ala-TIMP-1, had ~200-fold less activity toward MMP-9, whereas the activity toward MMP-7 was essentially abolished.[4]

Disulfide bonds enhance the stabilities of three-dimensional structure of a peptides and proteins. For endothelin family members, the disulfide bonds modulate a modest fraction of endothelin receptor binding and subsequent vasopressor activ-

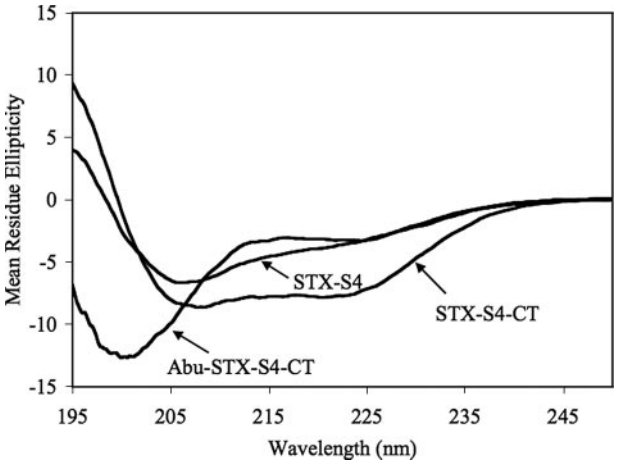

FIGURE 5. **Circular dichroism spectra of STX variants.** Circular dichroism spectra were recorded in the far UV range for 100 μM peptide dissolved in 20% enzyme buffer.

ity. The TIMP disulfide bonds are also important for stabilizing the three-dimensional structure necessary for inhibition, with Cys^1–Cys^{70} being the most critical for activity (11). To investigate the role of the disulfide bonds in MMP inhibitory activity in STX-S4-CT, a variant of STX-S4-CT sequence was synthesized with Cys^1, Cys^3, Cys^{11}, and Cys^{15} replaced by aminobutyric acid, which is a spatially comparable amino acid that is unable to form a disulfide. The Abu-STX-S4-CT peptide was synthesized, dissolved in folding buffer, purified, and tested for MMP inhibitory activity. This analog had very low activity as an MMP inhibitor (Table 2 and Fig. 4). A low level of activity remained in both Ac-STX-S4-CT and Abu-STX-S4-CT, but a peptide containing both modifications, AcAbu-STX-S4-CT, had virtually no inhibitory activity toward any of the enzymes tested (Table 2 and Fig. 4). A comparison of collagenase *versus* gelatinase inhibition profiles indicated that for MMP-1 the N-terminal α-amino group of Cys1 is more important for activity than the disulfide-bonded tertiary structure, whereas for MMP-2 and -9 the N-terminal charge was relatively less important for activity (Fig. 4).

Structural Characterization—After partial reduction of STX-S4-CT with tris(2-carboxyethyl) phosphine and derivatization with NEM, a modified form of the peptide was isolated by HPLC that eluted later than the native peptide and earlier than the fully reduced form. Sequence analysis indicated that Cys^1 and Cys^{15} alone were modified by NEM, indicating that Cys^3 and Cys^{11} are protected from NEM by disulfide bond formation so that the STX-S4-CT peptide retains the native Cys^1–Cys^{15}, and Cys^3–Cys^{11} connectivity. Each Srt variant was characterized with respect to secondary structure content by CD spectroscopy. The far UV CD spectra of STX and its Val^{16}, Ala^4, and Ser^4 variants (Fig. 5) resemble that of full-length Srt b (22, 45). Analysis of the CD spectra with the neural network program k2d (35) gives secondary structure contents for STX and its single site variants (Ala^4, Ser^4, and Val^{16}) of 8–10% α-helix and 36–44% β-structure; however, the spectra of STX-CT and STX-S4-CT suggest 20 and 30% helix and 27 and 13% β-structure, respectively. As expected, Abu-STX-S4-CT has a distinctly different solution structure compared with the disulfide-containing analogs (Fig. 5).

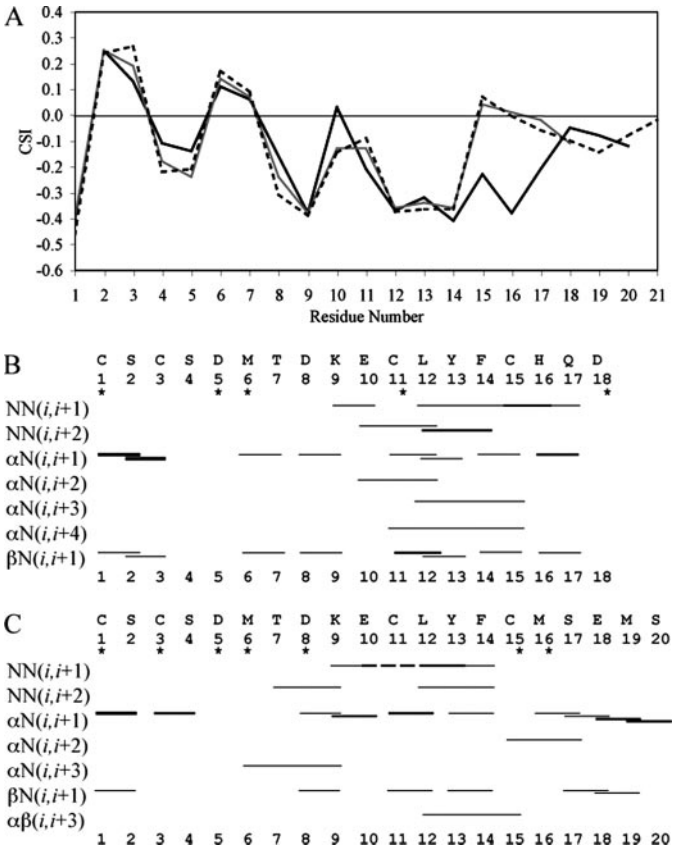

FIGURE 6. **NMR characterization of peptides:** *A*, α-proton chemical shift index is shown for Srt6b peptide (*black dashed line*), STX-S4 (*gray solid line*), and STX-S4-CT (*black solid line*). Sequential NOEs of STX-S4 and STX-S4-CT are shown in *B* and *C*, respectively. The intensity of the NOE is indicated by the *thickness* of the *line*. The *dotted line* indicates a region in which the NOE could not be unambiguously assigned because of similarity in NH chemical shift between Glu^{10} and Leu^{12}. The asterisks indicate NH protons not detected in the spectra (6).

Although the CD spectra suggest that the C-terminal TIMP-like extension enhances the α-helix content of the peptide, additional structural evidence is needed to determine whether this is correct and to determine which residues are responsible for the increased helicity. With this goal, we used nuclear magnetic resonance spectroscopy to further characterize the structure. Two-dimensional total correlation spectroscopy and NOE spectrometry spectra were obtained for STX-S4 and STX-S4-CT. Sequence-specific assignments were achieved for all α-CH protons, as well as the majority of amide protons. This allowed us to generate NOE-based secondary structure connectivity maps (Fig. 6, *B* and *C*). The chemical shift of the α-CH proton of an amino acid is more shielded when in a helical conformation and less shielded when in a β-strand extended conformation, with respect to the random coil value (48). This chemical shift index plot (Fig. 6*A*), indicates that the substitution of Ser at position 4 for Lys in Srt6B produces insignificant changes in secondary structure. However, the insertion of the TIMP-like C terminus in STX-4-CT extends the helical segment beyond that found in the original Srt6b or STX-S4. In addition, more NOEs are present in STX-S4-CT than in STX-S4, including a greater number of long range interactions. This indicates that STX-S4-CT is more structured than STX-S4, in agreement with the CD spectra (Fig. 5). This result is similar to the crystal struc-

tures of ET family members in which the C terminus is largely helical (6, 8, 45).

DISCUSSION

The development of specific low molecular weight inhibitors of metalloproteinases has been in progress for approximately two decades and has generated an array of molecules that are effective selective inhibitors *in vitro*, yet most have failed in clinical trials (49, 50). Hydrophobicity, which is often associated with high affinity binding to MMPs, can lead to membrane association and lower *in vivo* availability, whereas the presence of a potent zinc-binding moiety in most inhibitors may contribute to binding to zinc metalloproteins other than MMPs with the potential for deleterious side effects. Peptides and their derivatives are logical starting points for developing novel, less hydrophobic inhibitors of proteases, and structured peptides offer advantages over unstructured peptides because of lower entropic costs of binding. This appears to be an important principle in relation to ligand binding to metalloproteinases because previous studies have shown that substrate structure can have a major influence on substrate selectivity for different enzymes of this type (27). Members of the endothelin family of peptides have well defined tertiary structures stabilized by two disulfide bonds. Fortuitously, this fold has a marked similarity to the core of the MMP inhibitory site of the TIMPs, which in the four structurally characterized TIMP/MMP complexes makes the majority of contacts with the protease (14–17). This suggested the possibility that endothelin family members could be a starting point for developing a peptide-based metalloproteinase inhibitor. Previous studies have shown that removal of Trp21 of ET eliminated the vasoconstrictive activity (22, 51). In the present study, we have used as a starting point Srt6b variants with a truncated C terminus. Modifications have been introduced to optimize binding to and inhibition of MMPs. The generation of a "mini-TIMP" in this manner can provide a lead for designing selective MMP inhibitors that are less hydrophobic.

C-terminal deletions greatly reduce the MMP inhibitory activity, but this can be restored and improved by sequence substitution for residue 4 and an appropriate C-terminal extension. In the course of the present work, multiple substitutions have been made for residues 2, 4, and 16–21 of Srt6b. In all cases, the peptide folds and generates the native Cys^{1}–Cys^{15} and Cys^{3}–Cys^{11} disulfide bond pairing, highlighting the resilience of the Srt framework.

NMR and crystallographic studies of TIMP-1 and MMP-3 and their complex indicate that structural adjustments occur in both proteins upon complex formation (14–17, 52). In N-TIMP-1, structural changes in the A-B loop and C-D connector are thought to affect the ability of Val^{69} to make contact with the enzyme and optimize binding interactions between enzyme and inhibitor. Also, the residues that form the protein-protein interface become more rigid in the complex; these changes impart both enthalpic and entropic costs to complex formation. In the case of the MMP-binding ridge of N-TIMP-1, these costs have been estimated at 8–13 kcal/mol (52). Although a peptide inhibitor, such as a Srt analog, will have a smaller interaction surface for the MMP as compared with a protein inhibitor, it is possible that the thermodynamic costs of binding are less in the case of an appropriately designed constrained peptide.

FIGURE 7. **A model of a complex of STX-S4-CT with the catalytic domain of MMP-1.** The construction of the STX-S4-CT model and the docking procedure are described under "Discussion."

The STX-S4-CT inhibitor developed in the present study shows a marked improvement in affinity as compared with the initial truncated STX peptide as well as selectivity of binding to different MMPs. However, its usefulness as an inhibitor would be enhanced by further improvements in affinity and selectivity. Based on the fact that *N*-acetylation of STX-based inhibitors greatly reduces the MMP inhibitory activity, as well as the effects of substitutions for residue 4, it is reasonable to hypothesize that the STX variant interactions with MMPs are similar to those of TIMPs. We constructed a model of STX-S4-CT using the coordinates of the NMR solution structure of Srt b (model 10 of Protein Data Bank code 1SRB (45)) by substituting Ser at position 4, deleting the C-terminal hexapeptide (Fig. 1). We added the C-terminal Met-Ser-Glu-Met-Ser pentapeptide in α-helical conformation, based on information from CD and NMR studies (Figs. 5 and 6) of the solution structure and also conducted energy minimization using HyperChem. The PatchDock algorithm was used on-line (bioinfo3d.cs.tau.ac.il/PatchDock/) to predict docking sites with the catalytic domain of MMP-1 (53). A number of the predicted docking sites were distant from the active site of MMP-1, but one (solution 3; Fig. 7) is similar to the binding site for TIMP. In this projected complex, the N terminus of the inhibitor is within 3.5 Å of the catalytic Zn^{2+} ion, Asn^{171}–Phe^{174}, Asn^{180}, and Phe^{185} of

MMP-1. Additional contacts are between Ser^4 (inhibitor) and Leu^{181} (enzyme), Tyr^{210} (enzyme), and between Met^6 (inhibitor) and Gly^{179} (enzyme). Four inhibitory MMP-TIMP complexes have been structurally characterized by NMR and x-ray crystallography (14–17, 52). A comparison of these structures with our putative MMP-peptide interactions shows similarities together with differences in two areas. First, there are no direct contacts between the Srt variant and two zinc-coordinating His residues and the catalytic Glu^{219} in our model peptide-enzyme complex. Because it is within 5 Å of this region, contacts with this region might be enhanced by relatively minor structural adjustments in the inhibitor. Second, Ser^4 of the inhibitor is in contact with Tyr^{210} of the MMP. An equivalent interaction is not present in the TIMP-1/MMP-3 complex (14); however, in the recently determined structure of the N-TIMP-1/MMP-1 complex, Val^4 of the TIMP makes two contacts with Tyr^{210} of the MMP (16), suggesting that the model has some predictive value. Improving the contacts between enzyme and inhibitor in this region might offer a means of enhancing the selectivity of the inhibitor between different MMPs. The model of the STX-S4-CT:MMP-1 complex provides ideas about inhibitor-enzyme contacts that can be tested experimentally; it is consistent with the present data on structure-function relationships and, more importantly, offers direction for inhibitor optimization.

REFERENCES

1. Quinton, L., LeCaer, J. P., Phan, G., Lingny-Lemaire, C., Bourdais-Jomaron, J., Ducancel, F., and Chamot-Rooke, J. (2005) *Anal. Chem.* **77,** 6630–6639
2. Hayashi, M. A. F., Ligny-lemaire, C., Wollberg, Z., Wery, M., Galat, A., Ogawa, T., Muller, B. H., Lamthanh, H., Doljansky, Y., Bdolah, A., Stocklin, R., and Ducancel, F. (2004) *Peptides* **25,** 1243–1251
3. Fernandez-Patron, C., Radomski, M. W., and Davidge, S. T. (1999) *Circ. Res.* **85,** 906–911
4. Ducancel, F., Matre, V., Dupont, C., Lajeunesse, E., Wollberg, Z., Bdolah, A., Kochva, E., Boulain, J.-C., and Menez, A. (1993) *J. Biol. Chem.* **268,** 3052–3055
5. Cody, W. L., and Doherty, A. M. (1995) *Biopolymers* **37,** 89–104
6. Mills, R. G., Atkins, A. R., Harvey, T., Junius, F. K., Smith, R., and King, G. F. (1991) *FEBS Lett.* **282,** 247–252
7. Skolovsky, M., Galron, R., Kloog, Y., Bdolah, A., Indig, F. E., Blumberg, S., and Fleminger, G. (1990) *Proc. Natl. Acad. Sci. U. S. A.* **87,** 4702–4706
8. Janes, R. W., Peapus, D. H., and Wallace, B. A. (1994) *Nat. Struct. Biol.* **1,** 311–319
9. Abraham, D., Ponticos, M., and Nagase, H. (2005) *Curr. Vasc. Pharmacol.* **3,** 369–379
10. Gray, G. A., and Webb, D. J. (1996) *Pharmacol. Rev.* **72,** 109–148
11. Brew, K., Dinakarpandian, D., and Nagase, H. (2000) *Biochim Biophys Acta* **1477,** 267–283
12. Kashiwagi, M., Tortorella, M., Nagase, H., and Brew, K. (2001) *J. Biol. Chem.* **276,** 12501–12504
13. Wei, S., Chen, Y., Chung, L., Nagase, H., and Brew, K. (2003) *J. Biol. Chem.* **278,** 9831–9834
14. Gomis-Rüth, F. X., Maskos, K., Betz, M., Bergner, A., Huber, R., Suzuki, K., Yoshida, N., Nagase, H., Brew, K., Bourenkov, G. P., Bartunik, H., and Bode, W. (1997) *Nature* **389,** 77–81
15. Fernandez-Catalan, C., Bode, W., Huber, R., Turnk, D., Calvete, J. J., Lichte, A., Tschesche, H., and Maskos, K. (1997) *EMBO J.* **17,** 5238–5248
16. Maskos, K., Lang, R., Tschesche, H., and Bode, W. (2007) *J. Mol. Biol.* **366,** 1222–1231
17. Iyer, S., Wei, S., Brew, K., and Acharya, K. R. (2007) *J. Biol. Chem.* **282,** 364–371
18. Meng, Q., Malinovskii, V. A., Huang, W., Hu, Y., Chung, L., Nagase, H., Bode, W., Maskos, K., and Brew, K. (1999) *J. Biol. Chem.* **274,** 10184–10189
19. Nagase, H., Suzuki, K., Cawston, T. E., and Brew, K. (1997) *Biochem. J.* **325,** 163–167
20. Huang, W., Meng, Q., Suzuki, K., Nagase, H., and Brew, K. (1997) *J. Biol. Chem.* **272,** 22086–22091
21. Ramalingam, K., and Snyder, G. H. (1993) *Biochemistry* **32,** 11155–11161
22. Nakajima, K., Kumagaye, S.-i., Nishio, H., Kuroda, H., Watanabe, T. X., Kobayashi, Y., Tamaoki, H., Kimura, T., and Sakakibara, S. (1989) *J. Cardiovasc. Pharmacol.* **13,** S8–S12
23. Atkins, A. R., Ralston, G. B., and Smith, R. (1994) *Int. J. Peptide Protein Res.* **44,** 372–377
24. Aimoto, S., Hojoh, H., and Takasaki, C. (1990) *Biochem. Int.* **21,** 1051–1057
25. Knight, C. G., Willenbrock, F., and Murphy, G. (1992) *FEBS Lett.* **296,** 263–266
26. Nagase, H., Fields, C. G., and Fields, G. B. (1994) *J. Biol. Chem.* **269,** 20952–20957
27. Lauer-Fields, J. L., Minond, D., Sritharan, T., Kashiwagi, M., Nagase, H., and Fields, G. B. (2007) *J. Biol. Chem.* **282,** 142–150
28. Lauer-Fields, J. L., Broder, T., Sritharan, T., Nagase, H., and Fields, G. B. (2001) *Biochemistry* **40,** 5795–5803
29. King, D. S., Fields, C. G., and Fields, G. B. (1990) *Int. J. Pept. Protein Res.* **36,** 255–266
30. Ostresh, J. M., Winkle, J. H., Hamashin, V. T., and Houghten, R. A. (1994) *Biopolymers* **34,** 1681–1689
31. Lauer-Fields, J. L., Nagase, H., and Fields, G. B. (2000) *J. Chromatogr. A* **890,** 117–125
32. Ellman, G. L. (1959) *Arch. Biochem. Biophys.* **82,** 70–77
33. Bulaj, G., Kortemme, T., and Goldenberg, D. P. (1998) *Biochemistry* **37,** 8965–8972
34. van den Hooven, H., van den Burg, H. A., Vossen, P., Boeren, S., de Wit, P. J., and Vervoort, J. (2001) *Biochemistry* **40,** 3458–3466
35. Andrade, M. A., Chacon, P., Merelo, J. J., and Moran, F. (1993) *Protein Eng.* **6,** 383–390
36. Chung, L., Shimokawa, K., Dinakarpandian, D., Grams, F., Fields, G. B., and Nagase, H. (2000) *J. Biol. Chem.* **275,** 29610–29617
37. Itoh, Y., Binner, S., and Nagase, H. (1995) *Biochem. J.* **308,** 645–651
38. Huang, W., Suzuki, K., Nagase, H., Arumugam, S., Van Doren, S., and Brew, K. (1996) *FEBS Lett.* **384,** 155–161
39. Kashiwagi, M., Enghild, J. J., Gendron, C., Hughes, C., Caterson, B., Itoh, Y., and Nagase, H. (2004) *J. Biol. Chem.* **279,** 10109–10119
40. Hwang, T. L., and Shaka, A. J. (1995) *J. Magn. Reson. A* **112,** 275–279
41. Piotto, M., Saudek, V., and Sklenar, V. (1992) *J. Biomol. NMR* **2,** 661–665
42. Price, W. S. (1999) *Annu. Rep. NMR Spectroscopy* **38,** 289–354
43. States, D. J., Haberkorn, R. A., and Ruben, D. J. (1982) *J. Magn. Reson.* **48,** 286–292
44. Wüthrich, K. (1986) *NMR of Proteins and Nucleic Acids,* John Wiley & Sons, Inc., New York
45. Atkins, A., Martin, R. C., and Smith, R. (1995) *Biochemistry* **34,** 2026–2033
46. Troeberg, L., Tanaka, M., Wait, R., Shi, Y. E., Brew, K., and Nagase, H. (2002) *Biochemistry* **41,** 15025–15035
47. Higashi, S., and Miyazaki, K. (1999) *J. Biol. Chem.* **274,** 10497–10504
48. Wishart, D. S., Sykes, B. D., and Richards, F. M. (1992) *Biochemistry* **31,** 1647–1651
49. Coussens, L. M., Fingleton, B., and Matrisian, L. M. (2002) *Science* **295,** 2387–2392
50. Ramnath, N., and Creavan, P. J. (2004) *Curr. Oncol. Rep.* **6,** 96–102
51. Kimura, S., Kasuya, Y., Sawamura, T., Shinmi, O., Sugita, Y., Yanagisawa, M., Goto, K., and Masaki, T. (1988) *Biochem. Biophys. Res. Commun.* **156,** 1182–1186
52. Arumugam, S., Gao, G., Patton, B. L., Semenchenko, V., Brew, K., and Van Doren, S. R. (2003) *J. Mol. Biol.* **327,** 719–734
53. Schneidman-Duhovny, D., Inbar, Y., Polak, V., Shatsky, M., Halperin, I., Benyamini, H., Barzilai, A., Dror, O., Haspel, N., Nussinov, R., and Wolfson, H. J. (2003) *Proteins* **52,** 107–112
54. Pettersen, E. F., Goddard, T. D., Huang, C. C., Couch, G. S., Greenblatt, D. M., Meng, E. C., and Ferrin, T. E. (2004) *J. Comput. Chem.* **25,** 1605–1612